

Power Spectra to 1% Accuracy between Dynamical Dark Energy Cosmologies^{*}

Matthew J. Francis^{1†}, Geraint F. Lewis¹ and Eric V. Linder²

¹ *School of Physics, University of Sydney, NSW 2006, Australia*

² *University of California, Berkeley Lab, Berkeley, CA 94720, USA*

ABSTRACT

For dynamical dark energy cosmologies we carry out a series of N-body gravitational simulations, achieving percent level accuracy in the relative mass power spectra at any redshift. Such accuracy in the power spectrum is necessary for next generation cosmological mass probes. Our matching procedure reproduces the CMB distance to last scattering and delivers subpercent level power spectra at $z = 0$ and $z \approx 3$. We discuss the physical implications for probing dark energy with surveys of large scale structure.

Key words: methods:N-body simulations — methods: numerical — dark matter — dark energy — large-scale structure of Universe

1 INTRODUCTION

The mass power spectrum plays a central role in understanding the large scale structure of the Universe and the cosmic expansion affecting the development of structure. Cosmological probes of the growth history or the expansion history such as weak gravitational lensing, baryon acoustic oscillations, or galaxy/cluster abundances depend crucially on accurate knowledge of the mass power spectrum for physical interpretation of the data from large scale surveys.

Most commonly the mass power spectrum is approximated by the ‘Halofit’ form of Smith et al (2003), and this is used to determine cosmological parameters from the data (or estimate future precision of parameter extraction). However, the Smith et al (2003) formula is calibrated only on Λ CDM models, and for these has a precision of $\sim 10\%$. This will be insufficient for future large structure surveys that aim to explore the acceleration of the cosmic expansion and the properties of dark energy responsible for it. Huterer & Takada (2005) estimate that for weak gravitational lensing surveys, for example, 1% accuracy in knowledge of the mass power spectrum will be required.

N-body simulations provide a well-tested technique for calculating the dark matter power spectrum at the percent level (Heitmann et al 2005). While this treats purely gravitational forces, leaving out baryonic effects including heating and cooling, this should be a sufficient approximation for wavemodes $k < 3 h\text{Mpc}^{-1}$ (Jing et al. 2006; Zhan & Knox

2004; White 2004), or the scales larger than galaxies, that are of most relevance for large surveys. However, carrying out simulations for every possible cosmological model is obviously impractical. If one could devise a mapping procedure that matched models with the same key physical quantities, ideally to a single class of cosmologies like Λ CDM, then this would greatly aid the study of the cosmological information carried by the distribution and growth of large scale structure.

In Section 2 we outline the approach to such a mapping procedure and compare to previous work. Section 3 describes the details of the simulations performed and tests carried out. The qualitative physical consequences of the mapping are interpreted in Section 4. We present the computational results in Section 5 and identify several interesting features in the wavemode and redshift dependence of the power spectrum. Physical interpretation of these results are discussed in Section 6, with conclusions and future directions summarised in Section 7.

2 DARK ENERGY AND COSMIC STRUCTURE

While the influence of dark energy on the linear growth factor of matter density perturbations can be calculated simply (see below), the full, nonlinear mass power spectrum requires N-body simulations. Such simulation studies of the nonlinear power spectrum that exist for dark energy other than a cosmological constant have tended to be for a constant dark energy pressure to density ratio, or equation of state ratio w (Ma et al. 1999; White & Vale 2004; Linder & White 2005; McDonald et al 2006).

^{*} Research undertaken as part of the Commonwealth Cosmology Initiative (CCI: www.thecci.org), an international collaboration supported by the Australian Research Council

[†] Email: mfrancis@physics.usyd.edu.au

A few simulation studies have considered the effects of dynamical dark energy on the power spectrum, either through a parameterized time (or scale factor a) dependent form $w(a)$ or a specific scalar field potential (Klypin et al 2003; Macciò et al 2004; Ma 2006).

Efforts to calibrate non-linear power spectrum fitting formulas include early work by Ma et al. (1999), which was much improved upon with the advances in computing power by McDonald et al (2006). Both of these studies looked at modifying existing fits in the case of constant w cosmologies. Linder & White (2005) (LW) investigated the effects of w on the non-linear power spectrum, searching for key physical quantities, and discovered a simple matching prescription for calculating the non-linear mass power spectrum to within one to two percent.

This work extends the study of the dark energy effects on the full, non-linear mass power spectrum to models with dynamical dark energy, utilizing the model independent, physically motivated (Linder 2003) evolving equation of state $w(a) = w_0 + w_a(1 - a)$. At the same time, we employ the approach of seeking central physical matching quantities that incorporate CMB data through agreeing on the distance to the last scattering surface.

In studying the non-linear power spectrum of mass fluctuations, a natural place to start is with the linear power spectrum. The effects of dark energy on the linear mass power spectrum can be calculated through the relation

$$P(k, a) = \frac{D^2(a)}{D^2(a_i)} P(k, a_i) \quad (1)$$

(see e.g. Coles & Lucchin (2002)) with the growth factor $D(a)$ given by the formula (e.g. Hu (2002); Linder & Jenkins (2003))

$$D'' + \frac{3}{2} \left[1 - \frac{w(a)}{1 + X(a)} \right] \frac{D'}{a} - \frac{3}{2} \frac{X(a)}{1 + X(a)} \frac{D}{a^2} = 0 \quad (2)$$

with derivatives with respect to scale factor a , and where $X(a)$ is the ratio of the matter to dark energy densities, given by $X(a) = \frac{\Omega_m}{1 - \Omega_m} e^{-3 \int_a^1 \frac{da'}{a' w(a')}}$, with Ω_m the dimensionless present matter density.

The non-linear power spectrum cannot be written in terms of a simple differential equation and requires the use of large volume, high resolution, N-body simulations. These are computationally expensive and therefore accurate semi-analytic fitting formulas derived from simulation results are a valuable tool. The most widely adopted current formula, sometimes called Halofit, was presented in Smith et al (2003). This formula is motivated by the halo model of structure growth with free parameters in the function set by fitting to a large suite of simulations. All these simulations, however, were of cosmological constant, $w = -1$, cosmologies. McDonald et al (2006) produced a fitting formula as a multipolynomial series for constant w models, intended to be used to modify the Smith et al result. This modification was estimated to be accurate to within a few percent in the range of cosmologies encompassed by the simulation grid.

Taking a different approach, LW demonstrated that when the *linear* growth factors between different $w = \text{const}$ models were matched at a high redshift point as well as at $z = 0$, by compensating with other cosmological parameters, the *non-linear* power spectrum from N-body simulations also matched to much better than a percent at those red-

shifts, as well as matching to one to two percent at any intermediate redshift. Additionally, LW also found that the distance to the surface of last scattering, d_{ls} , closely matched when their growth matching criteria was implemented, preserving CMB constraints. With this formalism the power spectrum for a dark energy model can be matched to, say, a Λ CDM cosmology. Hence one can either use an appropriately matched Halofit result or carry out a vastly reduced suite of only Λ CDM simulations to achieve the desired accuracy on the mass power spectrum.

This article concentrates on developing accurate matching of the non-linear mass power spectrum for dynamical dark energy models. We employ a somewhat different matching procedure from LW, explicitly matching the distance to CMB last scattering d_{ls} and the mass fluctuation amplitude σ_8 at the present and studying the effect on the growth. In this respect, our approach is essentially the converse of the LW approach. The geometric factor of the distance to CMB last scattering suffices to incorporate substantially the CMB constraints on the dark energy parameters. Since dark energy had a negligible density in the early universe (except in special, early dark energy models, e.g. see Wetterich (2004); Doran & Robbers (2006); Linder (2006)), the physical size and nature of features in the CMB at the surface of last scattering is largely insensitive to the properties of dark energy. However, the angular size of such features is set through the angular diameter distance, which does depend on the properties of dark energy, since it relates to the expansion history of the universe $a(t)$. Therefore, dark energy models giving the same distance to the last scattering surface are largely degenerate with respect to the CMB (some differences relating to secondary anisotropies such as the ISW effect remain, see Hu & Dodelson (2002)). For a given dynamic dark energy model (w_0, w_a), there is a corresponding constant equation of state w_{eff} , say, that gives the same d_{ls} as the dynamical model, holding all other cosmological parameters (such as the physical matter density $\Omega_m h^2$) fixed. This article examines the relation between the non-linear mass power spectra of the dynamical and the w_{eff} models. Once a tight correspondence is established, one can then either employ a constant w fitting formula such as from McDonald et al (2006), carry out only a suite of constant w simulations, or adjust the other cosmological parameters such that one chooses $w_{\text{eff}} = -1$ and requires only Λ CDM simulations. We discuss these alternatives further in §7.

3 SIMULATION DETAILS

The simulations were performed using the GADGET-2 N-body code (Springel 2005), modified to incorporate the background evolution $a(t)$ appropriate for dynamical dark energy cosmologies with $w(a) = w_0 + (1 - a)w_a$. Fiducial simulation runs use 256^3 dark matter particles in a $256 h^{-1} \text{Mpc}$ periodic box with a 512^3 force grid; the initial redshift was $z = 24$ and the force softening was set to a constant comoving length of $60 h^{-1} \text{Kpc}$. In order to check numerical convergence, runs were also performed with combinations of box size and particle number a factor of 2 greater and smaller than the fiducial. In addition, runs checking convergence were performed for numerical parameters including the start time, softening length, PM grid spacing, time and

force accuracy and tree update frequency. The ratio of power between the different dark energy models were largely insensitive to these parameters, changing by a small fraction of a percent out to $k < 3 h\text{Mpc}^{-1}$.

The linear matter power spectra used to create the initial conditions were calculated using CAMB (Lewis, Challinor & Lasenby 2000). Initial conditions were generated from the power spectrum using part of the GRAFIC program within the COSMICS package (Ma & Bertschinger 1995).

For each set of distance-matched runs, the same input power spectrum, generated by CAMB using the $w = \text{constant}$ model, was used for each model. In order to match the amplitude of linear growth today (identical σ_8 at $z = 0$) for simulations of different cosmologies, the initial density and velocity perturbations of the particles were scaled in the Zel'dovich approximation using the linear growth factor ratio $D(a_{\text{start}})/D(a = 1)$ for the different models. This ansatz for initial conditions is robust as long as the dark energy does not change the shape of the linear power spectrum at z_{start} , i.e. the dark energy plays little role in the very early universe. We have verified this to high accuracy using a version of CAMB modified for (w_0, w_a) models without dark energy perturbations. Note that in the presence of dark energy perturbations, the initial power spectrum over our range of $k = 0.1 - 3 h\text{Mpc}^{-1}$ is affected by less than 1% for constant w models that are *not* distance matched. We expect that distance-matched (w_0, w_a) models with perturbations will show less effect but future work will address this.

The calculation of the power spectrum in simulations outputs used the ‘chaining the power’ method described in Smith et al (2003) utilising the cloud in a cell assignment scheme. No correction was made for shot noise, as the quantity of interest was the ratio of the power between different models. See McDonald et al (2006) for an extended discussion of the usefulness of taking power spectrum ratios to eliminate many numerical errors in this type of study. See also White (2005).

All simulations in this paper used the best fit cosmological parameters from Spergel et al (2006) of $\Omega_m = 0.234$, $h = 0.74$, $\Omega_b = 0.0407$ and $\sigma_8 = 0.76$ in a flat ΛCDM universe. For each set of simulations, a constant equation of state w_{eff} is selected and several values for the parameters w_0 and w_a that maintained the same d_{ISS} were calculated. One consequence of this methodology is that these $w(a)$ models cross the value $w = -1$ at some point in cosmic history. Debate exists surrounding the physical validity of crossing between the phantom regime, defined as $w < -1$, and $w > -1$. This will eventually be settled by a microphysical theory for dark energy, rather than merely a phenomenological description. With this in mind we do not consider the issue of phantom energy and phantom crossing further.

We select three values, $w_{\text{eff}} = -0.9, -1, -1.1$, as the foundations for our comparison of $w(a)$ cosmologies. This range is in accord with constraints on constant w from current cosmological data sets (Spergel et al 2006; Seljak, Slosar, & McDonald 2006) and provides a reasonable variety for testing the matching procedure. For each constant w model, simulations were carried out for four more $w(a)$ models with matching distance to the LSS. The dark energy models used are summarized in Table 1.

$w_{\text{eff}} = -0.9$		$w_{\text{eff}} = -1.0$		$w_{\text{eff}} = -1.1$	
w_0	w_a	w_0	w_a	w_0	w_a
-1.1	0.620	-1.2	0.663	-1.3	0.707
-1.0	0.319	-1.1	0.341	-1.2	0.363
-0.8	-0.336	-0.9	-0.359	-1.0	-0.381
-0.7	-0.686	-0.8	-0.732	-0.9	-0.778

Table 1. Distance Matched Models. Simulations were carried out for five models (including $w = w_{\text{eff}}$) for each of three values of w_{eff} , where all five models in a column had identical distances to CMB last scattering.

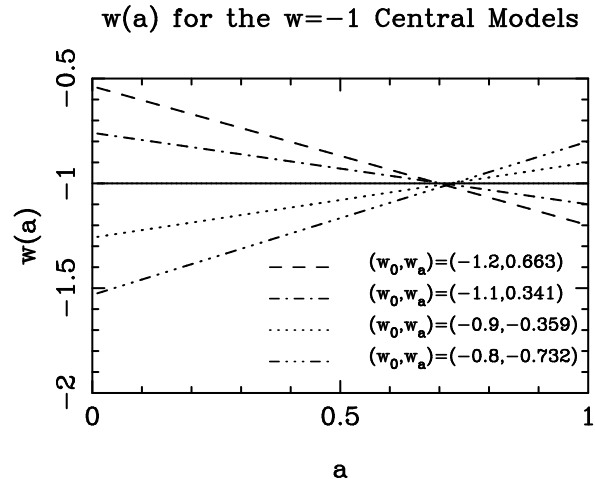


Figure 1. Dark energy equation of state vs. a for the models matched to the CMB last scattering surface distance for $w = -1$.

4 THE CONSEQUENCES OF DISTANCE MATCHING

If the simple distance matching procedure outlined in this paper is to succeed in producing a good match in the matter power spectrum, it might be expected to keep a range of physical conditions similar through cosmic history. This is indeed what is found. In particular, a variety of physical quantities exhibit pivot or crossover points, indicating not only near equality at that epoch, but a tendency toward agreement of quantities integrated over cosmic history. For instance, Figure 1 plots $w(a)$ for the four models with matching distance to the $w = -1$ model; there is a clear epoch at $a \approx 0.7$ where the values all cross $w = -1$.

The linear growth factors of the various distance matched models also closely track each other. While the linear growth is matched at $a = 1$ by construction, there is an additional epoch at high redshift where the linear growth of all associated models closely matches. For the $w_{\text{eff}} = -1$ set of models shown in Figure 2, the matching point is $a = 0.24$ or $z = 3.12$. The other two sets of models match at a similar value and show a similar trend. This behaviour illustrates the converse of what was found in LW, where d_{ISS} was found to closely match when the linear growth was matched at some high redshift point. The crossover is important, since rather than all models diverging from the $z = 0$ match,

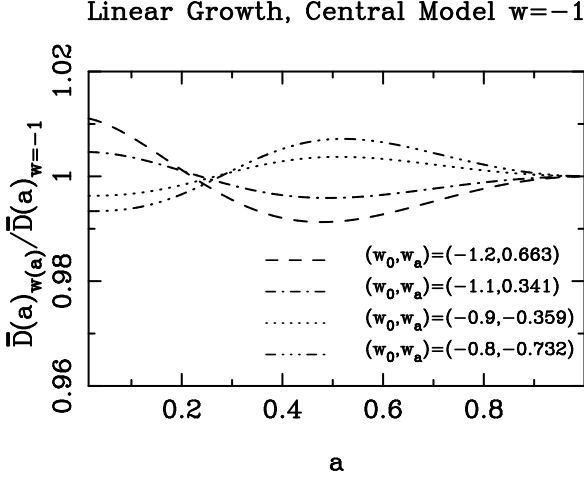


Figure 2. Ratio of the linear growth factor $\bar{D}(a) \equiv D(a)/D(1)$ relative to the central $w = -1$ model for the $w(a)$ models with matched d_{ISS} .

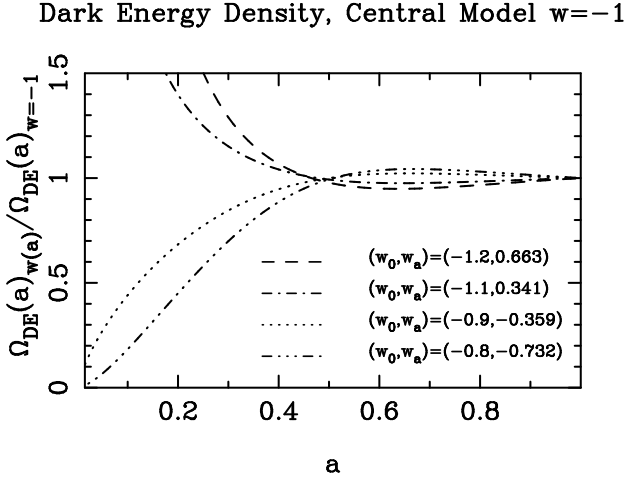


Figure 3. Ratio of $\Omega_{\text{DE}}(a)$ relative to the central $w = -1$ model for the $w(a)$ models with matched d_{ISS} .

the curves track each other relatively closely. Since the non-linear power spectrum is intimately tied to the linear behavior, this provides hope that a mapping of the full power spectrum between models can be realized.

The growth crossover behaviour results from a change in sign of the relative rate of growth at $a \approx 0.5$. In the linear regime the growth of fluctuations can be seen as a balance between the mutual gravitational attraction of the overdensity, which is amplified by higher mean matter density, and the expansion rate of the universe characterised by $H(a)$, which acts like a frictional term, suppressing growth the higher the expansion rate. In this picture, greater relative matter domination at a particular epoch will produce a more rapid growth rate at that time compared to a less matter dominated model. With this in mind it is worth comparing the matter domination history of our suite of cosmologies. Figure 3 shows the relative dark energy density $\Omega_{\text{de}}(a)$ for the $w(a)$ models matched to $w = -1$.

Comparing figures 2 and 3 we see that where the relative dark energy density is higher, the relative rate of linear growth is lower. For instance, the long dashed model has a

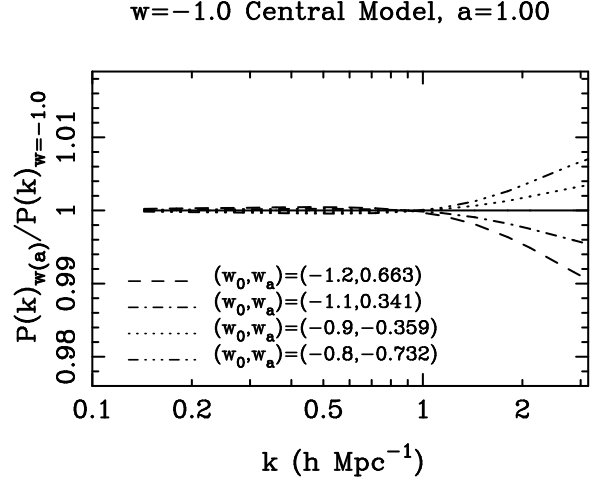


Figure 4. Ratio of the non-linear mass power spectrum at $z=0$ relative to the $w = -1$ model for models with matched d_{ISS} .

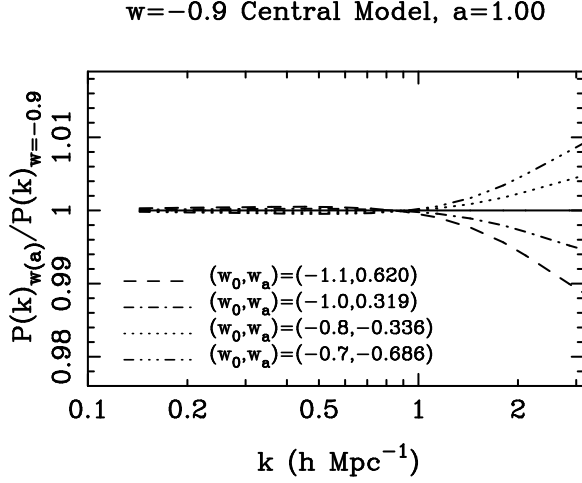
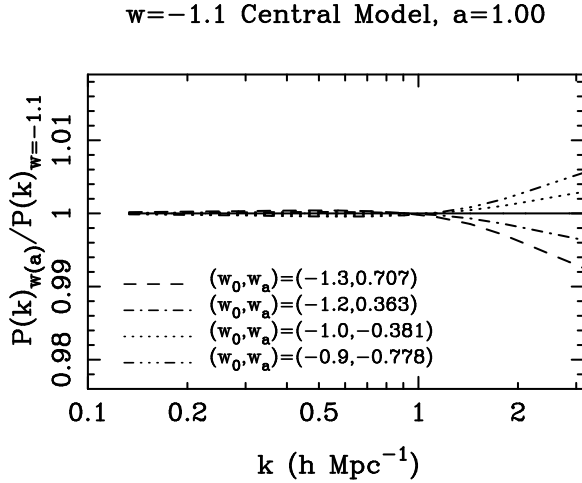
more negative slope in the region $a < 0.5$ in figure 2 than the other models, corresponding to a higher relative dark energy density in this region as shown in figure 3. The magnitude of growth is greater initially in the long dashed model in order to achieve the match at $z = 0$, however the growth initially grows more slowly in comparison to the other models. The change in sign of the relative growth rates at $a \approx 0.5$ in figure 2 corresponds to the crossover point in relative matter domination in Figure 3. The energy density, like the linear growth, exhibits a striking crossover point, again keeping physical conditions similar between models throughout cosmic history.

In a chain of related conditions, the crossover point of the equation of state $w(a)$ (see Figure 1) causes the convergence of the dark energy density $\Omega_{\text{de}}(a)$ (see Figure 3, and the crossover of $\Omega_{\text{de}}(a)$ leads to the convergence of the growth $D(a)$ (see Figure 2), which then creates a crossover in the growth at higher redshift. This in turn will keep the non-linear power spectrum closely matched between the models over the entire range $z = 0 - 3$.

5 RESULTS

The ratio of power measured in the simulation outputs at $z = 0$ relative to the central w_{eff} model for each of the sets of simulations is given in Figures 4, 5 and 6. The most outstanding result is the excellent agreement between the mapped power spectra, at the 0.1% level for $k < 1 \text{ hMpc}^{-1}$ and $\lesssim 1\%$ for $k < 3 \text{ hMpc}^{-1}$ ($\lesssim 0.5\%$ at the higher k for the less rapidly varying dark energy models). These figures show very similar trends, regardless of the fiducial w_{eff} model chosen. Since the trends are similar, the remaining figures will show the results for the $w = -1$ central models only, for brevity.

The simulations shown in these figures started with an identical realisation of initial conditions, albeit scaled with respect to the linear growth factor to produce matched linear growth at $z = 0$. As the deviations between models are small, it is important to take care to ensure that any features are real and not the results of a spurious numerical effect.

Figure 5. As Fig. 4, for the central model $w = -0.9$.Figure 6. As Fig. 4, for the central model $w = -1.1$.

The convergence tests described in Section 3 addressed the effects of numerical parameters¹.

There are also two other potential sources of error, the limited volume of the simulation box and the error sampling error in calculating the power spectrum of the simulation snapshots. Care must be taken that these effects are not causing spurious results. Figure 7 shows the results for the $w = -1$ central model simulations with rms sampling errors from the FFT power spectrum calculation plotted. For clarity these have been omitted from the other plots, however the errors are similar in all cases.

From this plot the deviation between models is roughly

¹ Changing particle resolution did cause a slight systematic shift in features seen in the power spectrum ratios. The onset of the dispersion between the models seen in figures 4-6 at $k \sim 1 h\text{Mpc}^{-1}$ shifted to lower k with reduced particle resolution and higher k with an increase. This shift was of order 0.1 in $\log k$ for factors of two differences in particle resolution. We cannot fully account for this numerical effect, however the difference in power at a given k -mode due to the shift is at most $\sim 0.1\%$ and since subpercent effects are beyond the ability of N -body simulations to probe accurately, we do not believe this effect is of significant consequence.

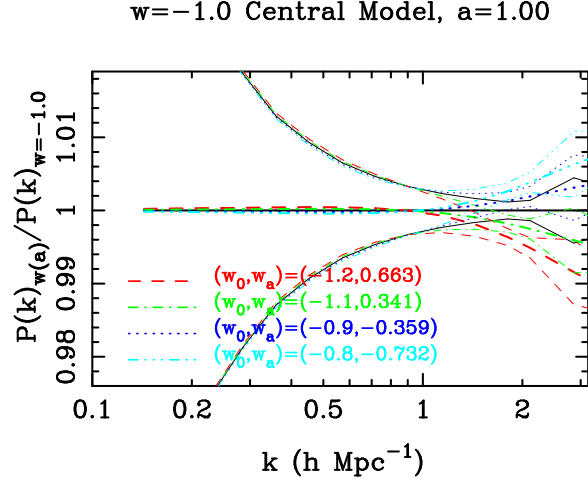


Figure 7. As Fig. 4, with rms sampling errors included, shown by thin lines of the same line style as each model.

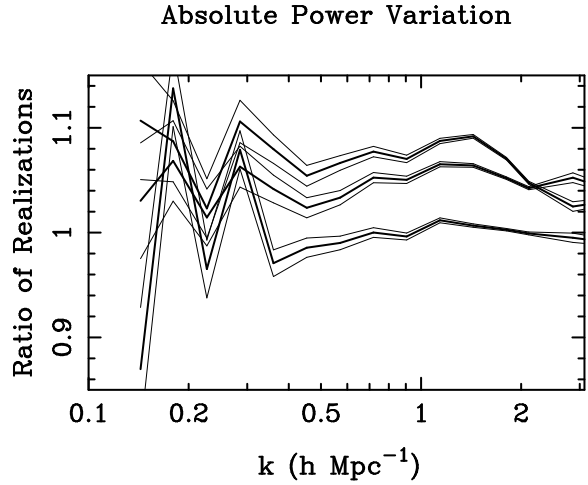


Figure 8. The effect on the power spectrum due to different realisations. Displayed are the power in three realisations of a single cosmological model, $w = -1$, as a ratio to the power in a fourth realisation. The rms errors for each power spectrum calculation are also shown. As expected the finite volume error decreases as k increases due to the greater number of modes present at higher wavenumbers.

a factor of 1–2 that of the rms error. In order to verify that the effects seen are genuinely due to the difference in dark energy models, another three sets of simulations with the same parameters but different realisations were performed. The scatter in the calculated power spectrum due to different realisations is shown in Figure 8. The scatter in this figure clearly demonstrates the inability to accurately determine the absolute power with the box sizes and number of realisations used in this study due to finite volume errors.

From the figures shown it is clear that the difference between realisations for a single cosmological model is greater than the difference within a single realisation for the different models. This makes accurate modeling of the absolute value of the power spectrum an extremely challenging task, requiring larger boxes, many more realisations and highly detailed consideration of sources of numerical error. Instead, we are interested in the effect of dark energy models relative

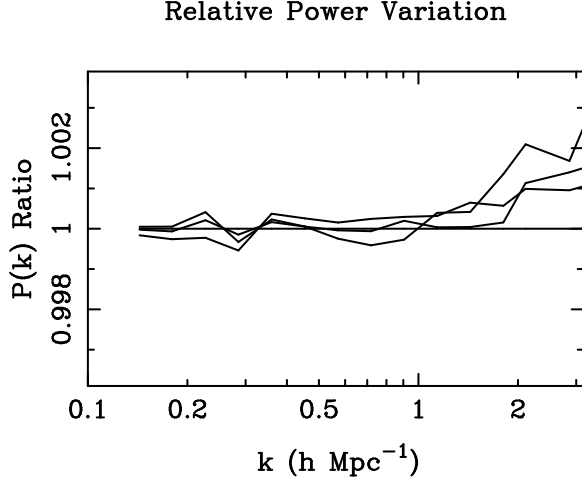


Figure 9. The effect of different realisations on the ratio of a dynamical dark energy power spectrum to the associated $w = \text{const}$ model. Shown are 4 realisations of the ratio between the strongly time varying $(w_0, w_a) = (-1.2, 0.663)$ model and the $w = -1$ model at $z = 1$, plotted as a ratio of the main realisation used in the paper. This is a typical example of the magnitude of the variation due to different realisations.

to one another and therefore what is important is how much the *ratios* between models (such as shown in Figures 4-6) are affected by different realisations. Fortunately the effect of different realisations is vanishingly small as seen in Figure 9, which shows a typical example of the variation in power ratios across the four realisations used.

From Figure 9 we can be confident that the computed non-linear power spectra ratios are not visibly affected by spurious finite volume errors or effects due to the FFT calculation of the power spectrum.

For cosmological structure probes, we are interested not just in how well we can predict the power spectrum at $z = 0$ but across all redshifts. In the simulations performed, data was output at a number of times. From Figure 2, two epochs are of particular interest. The first is the crossover in linear growth at $a = 0.24$ and the second is at $a = 0.5$ where the linear growth is most varied between models. The latter corresponds to $z = 1$, which is extremely relevant to a number of forthcoming cosmological surveys. Hence an accurate estimation of power here, provided by the distance matching scheme, is of great importance for understanding possible constraints on dark energy cosmologies.

The ratio of power measured in the simulations boxes at these epochs are shown in Figures 10 and 11.

We can do even better, however, by realizing that much of the difference in power, particularly at $a \approx 0.5$, can be accounted for by the difference in linear power. Scaling this out via Equation 1, the results are as shown in Figures 12 and 13.

From these figures we can see that the combined distance and growth matching procedure is generally accurate to better than 1%. The greatest deviation found in all simulation outputs is 2% for $k \approx 3 h\text{Mpc}^{-1}$ at $a = 0.5$.

Since the results shown thus far display a good match for distance matched models, it is worth considering how much improvement this matching achieves compared to arbitrary dark energy models that are not distance matched.

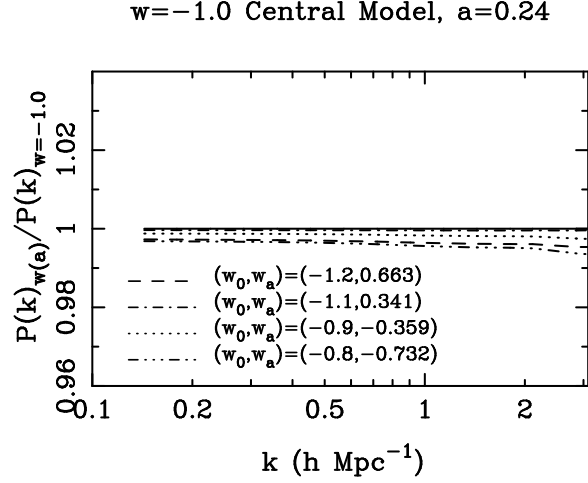


Figure 10. As Fig. 4, but at $a = 0.24$ where from Fig. 2 the linear growths closely match (slightly lower than for $w = -1$).

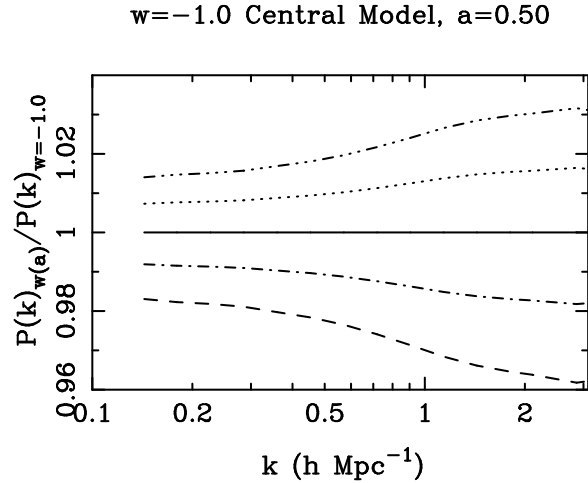


Figure 11. As Fig. 4, but at $a = 0.5$ where from Fig. 2 the linear growths are most divergent. Much of the difference in power comes from this difference in linear power.

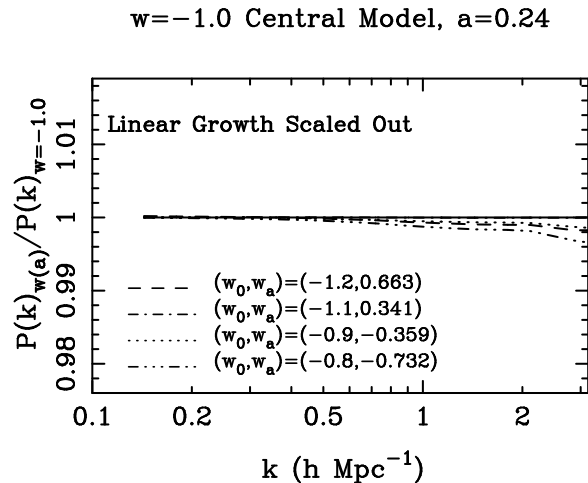


Figure 12. As Fig. 10, but with the linear growth difference scaled out. Note the reduced y-axis scale relative to Fig. 10.

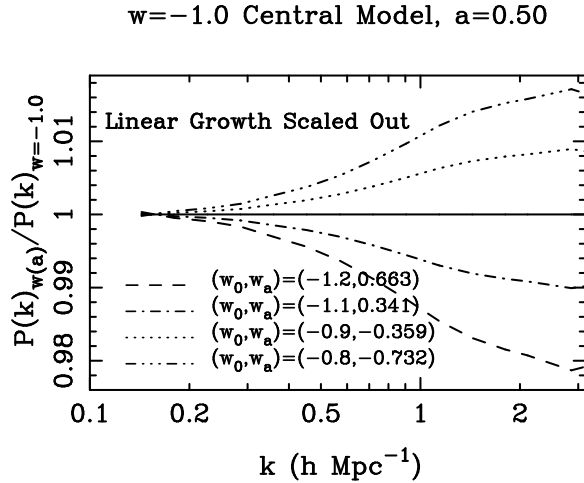


Figure 13. As Fig. 11, but with the linear growth difference scaled out. Note the reduced y-axis scale relative to Fig. 11.

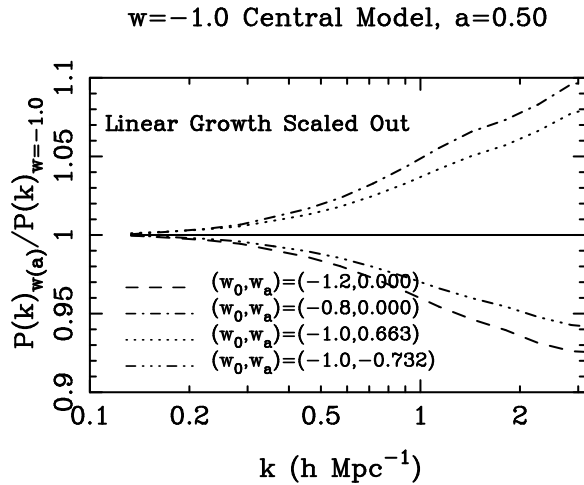


Figure 14. The ratio of the non-linear power in several non-distance matched cosmologies to a Λ CDM model at $z = 1$. The amplitude of linear growth at $z = 0$ is the same for all models as in previous figures. Note that the divergence between models increases with k but that the divergence begins at a lower k and is significantly greater than with the distance matched models shown previously

In other words, how much of a role do the values of the dark energy parameters play in structure formation, if all other parameters are kept fixed? Figure 14 shows the ratio of power at $z = 1$ between a Λ CDM model and several non-distance matched models with the same linear growth amplitude at $z = 0$. The divergence between these models is significantly greater than what is seen in the distance matched models (and of course they will disagree on the CMB), illustrating the improvement achieved by this simple scheme.

6 EVOLVING DARK ENERGY AND STRUCTURE GROWTH

The matching prescription used in this article produces a mapping between the matter power spectra of dark energy

cosmologies accurate to $\lesssim 1\%$ over a wide range of wave-modes and a wide range of cosmic history. This agreement 1) indicates that simple physical quantities determine the nonlinear power spectrum over this range, leading to the prospect of understanding structure formation on a fundamental level even in dynamical dark energy cosmologies, 2) points the way to significant advances in computational efficiency by reducing the dimension of the grid of simulations necessary to produce accurate estimations of power spectra required for interpretation of cosmological probes such as weak gravitational lensing, baryon acoustic oscillation, and other large scale structure surveys, and 3) identifies a degeneracy that makes it difficult to distinguish between models lying on a particular subsurface of the cosmological parameter space.

To try to ameliorate the degeneracy, we note that an evolving equation of state does imprint a small but systematic effect on the non-linear matter power spectrum. The general trend shown by Figures 4, 5 and 6 is that dark energy with a less negative value today but more negative value at high redshift (i.e. negative w_a) gives greater non-linear power at $k \gtrsim 1 h\text{Mpc}^{-1}$ than its d_{ISS} -matched w_{eff} model. Similarly, more negative equations of state today with positive w_a possess less power in the same range. This deviation is however relatively small, remaining less than 2% out to $k = 3 h\text{Mpc}^{-1}$. Even so, this partial degeneracy is not too worrying since it can readily be broken by other cosmological dependencies (e.g. the geometric distance dependence entering with the mass power spectrum into the weak lensing shear power spectrum or the baryon acoustic scale) or by complementary cosmological probes. Thus the model mapping technique does not appear to have any real drawbacks to detract from its physical and computational advantages.

Elaborating on the physical import of the mapping, a striking feature is the marked difference at $z = 0$ between $k < 1 h\text{Mpc}^{-1}$ where the power spectra between models match extremely closely and $k > 1 h\text{Mpc}^{-1}$ where they diverge. This seems to suggest a transition between the linear region at low k where by design the power should be matched, and the fully non-linear region at high k where differences in cosmic evolution have imprinted a different signature on the growth of structure on small scales, perhaps reflecting the effect of dark energy on conditions when structure formed at high redshift.

Those models that show a greater non-linear growth are those that in the early universe had a greater contribution of the matter density relative to the dark energy density; these correspond to the models with today $w_0 > w_{\text{eff}}$ and in the recent universe had *lower* matter density relative to dark energy density. This suggests that non-linear growth is more sensitive to conditions (including the effects of dark energy) in the early, matter dominated universe than it is to conditions in the later, accelerated era of dark energy domination.

Carrying this forward, one conjecture is that the “transition” in the behavior of the $z = 0$ power spectrum at $k = 1 h\text{Mpc}^{-1}$ might be related to early, rather than $z = 0$, non-linear effects. While the non-linear scale at $z = 0$ should be near $k \lesssim 0.2$, the power spectrum remains well matched here, possibly because the non-linear growth was already matched as a result of the model mapping, i.e. “pinned down” by the agreement at $a = 0.24$. So the greatest dif-

ference in non-linear growth, arising from times earlier than the $a = 0.24$ matching, might appear at the non-linear scale associated with $a < 0.24$, or $k \gtrsim 1 h\text{Mpc}^{-1}$, rather than the $z = 0$ non-linear scale. In any case, the accurate approximation of the power spectrum utilizing the matching prescription indicates that reasonably simple physics lies behind even the non-linear mass power spectrum.

7 CONCLUSION

The mass power spectrum lies at the foundation of many cosmological observables, such as the weak lensing shear statistics of galaxies, the large scale structure clustering distribution (including baryon acoustic oscillations), and cluster abundances. To utilize any of these cosmological measurements as next generation probes of large scale structure, cosmology, or dark energy requires clear and accurate understanding of the mass power spectrum over the range of models under consideration, e.g. dynamical dark energy not just ΛCDM .

The main results of this article (see Figs. 4,12 and 13) demonstrate that non-linear mass power spectra of dynamical dark energy models with smooth equation of state evolution can be determined to percent accuracy by calculating the power for the constant equation of state cosmology that gives a matching distance to the CMB last scattering surface. By varying other parameters as well, such as the matter density Ω_m and h keeping $\Omega_m h^2$ constant (see LW), one can envision mapping a wide variety of dark energy models to ΛCDM models, resulting in significant gains in computational efficiency. This can also alleviate concerns regarding phantom crossing.

Finding the distance matched models as described in this paper is a trivial task numerically requiring the integration of a differential equation and a one dimensional parameter search. This simple procedure however provides a mapping that is accurate to a percent. Of course the accuracy of the resultant power spectrum estimation is ultimately only as good as the accuracy in the model being mapped to. For that model we can then utilise fitting formulas, such as Halofit, for a rough, $\sim 10\%$ accuracy or more generally perform N-body simulations with the desired parameters. However, the distance matching scheme in this case allows a much reduced grid of simulations to be carried out while still maintaining a high degree of accuracy.

The physics behind the matching prescription involves a chain of consequences from the crossover in the behavior of one variable (e.g. equation of state) to the convergence in another, then leading to matching in the large scale structure growth. Further physics, not yet fully elucidated, points to the full nonlinear power spectrum being dependent not on the linear growth, but the linear growth *history*, where the conditions (e.g. matter density or growth factor) at one epoch directly manifest in the nonlinear behavior at a later epoch.

Future work should pursue this further, as well as investigating the prospects for discerning the signatures of more complicated equations of state or perturbations. While the prescription here for mapping the mass power spectrum to percent accuracy between cosmologies is useful in itself and for computational gains, the most exciting prospects are for

improved analytic fitting formulas and deeper physical understanding.

ACKNOWLEDGMENTS

MF acknowledges the support of a Science Faculty UPA, thanks Chris Power and Jeremy Bailin for helpful discussions, advice and pieces of code, and thanks LBNL and SNAP for hospitality and support during much of the writing of this article. We thank Martin White for pointing out the nice method of getting high resolution FFT's without needing large arrays and for other useful discussions. This work has been supported by the Australian Research Council under grant DP 0665574 and in part by the Director, Office of Science, US Department of Energy under grant DE-AC02-05CH11231.

REFERENCES

- “Cosmology: The origin and evolution of cosmic structure”
Coles P. & Lucchin, F., Wiley & Sons (Textbook)
- Hawkins, E. et al, 2003, MNRAS, 346, 78
- Dolag, K. et al, 2004, A&A, 416, 853
- Doran, M. & Robbers, G., 2006, JCAP, 0606, 026
- Heitmann, K., Ricker, P., Warren, M., & Habib, S., 2005, ApJS, 160 28
- Hu, W. 2002, PhRvD, 66, 083515
- Hu W. & Dodelson S., 2002, ARA&A, 40, 171
- Huterer, D., & Takada, M. 2005, Astroparticle Physics, 23, 369
- Jing, Y. P., Zhang, P., Lin, W. P., Gao, L., & Springel, V. 2006, ApJL, 640, L119
- Klypin A, Macciò, A., Mainini, R., & Bonometto, S., 2003, ApJ, 599, 31
- Knop R. et al, 2003, ApJ, 598, 102
- Kuhlen M. et al, 2005, MNRAS, 357, 387
- Lewis A., Challinor A. & Lasenby A., 2000, ApJ, 538, 473
- Linder E., 2003, PhRvL, 90, 9, 1301
- Linder E., 2006, Astroparticle Physics 26, 16
- Linder E. & Jenkins A., 2003, MNRAS, 346, 573
- Linder E. & White M., 2005, Phys Rev D 72, 061304(R)
- Ma, Z. 2006, ArXiv Astrophysics e-prints, arXiv:astro-ph/0610213
- Ma C. & Bertschinger E., 1995, ApJ, 455, 7
- Ma, C.-P., Caldwell, R. R., Bode, P., & Wang, L. 1999, ApJL, 521, L1
- Macciò A. et al, 2004, Phys. Rev. D 69, 123516
- McDonald P., Trac H. & Contaldi C., 2006, MNRAS, 366, 547
- Riess, A. et al, 2004, ApJ, 607, 665
- Seljak, U., Slosar, A., & McDonald P., 2006, JCAP 0610, 014
- Smith, R.E., et al. 2003, MNRAS, 341, 1311
- Solevi, P. et al, 2006, MNRAS, 366, 1346
- Spergel D. et al, astro-ph/0603449
- Springel V., 2005, MNRAS, 364, 110
- Wetterich, C. 2004, Phys. Lett. B, 594, 17
- White, M. 2004, Astroparticle Physics, 22, 211
- White, M. 2005, Astroparticle Physics, 24, 334
- White, M., & Vale, C. 2004, Astroparticle Physics, 22, 19

Zhan, H., & Knox, L. 2004, ApJL, 616, L75

This paper has been typeset from a \TeX / \LaTeX file prepared by the author.